

## Article

# Feasibility Study of Exhaust Energy Recovery System for Mobile Carbon Capture Operations in Commercial Engines through 1D Simulation

Seungchul Woo <sup>1</sup>, Yusin Jeong <sup>1</sup> and Kihyung Lee <sup>2,\*</sup>

<sup>1</sup> Department of Mechanical Engineering, Hanyang University, Ansan 15588, Gyeonggi, Republic of Korea; wooosc@hanyang.ac.kr (S.W.); jys9917@hanyang.ac.kr (Y.J.)

<sup>2</sup> Department of Mechanical Engineering, BK21 FOUR ERICA-ACE Center, Hanyang University, Ansan 15588, Gyeonggi, Republic of Korea

\* Correspondence: hylee@hanyang.ac.kr

**Abstract:** The global proportion of eco-friendly vehicles continues to increase; however, regarding hybrid vehicles, the vehicle powertrains in most countries include internal combustion engines. Therefore, research on reducing the carbon emissions from internal combustion engines must be conducted. Carbon capture technology must be developed for e-fuel, which has recently attracted attention, to achieve carbon neutrality. In this study, a turbo compound system capable of recovering waste exhaust gas energy was selected as the most appropriate energy supply system to operate a mobile carbon capture system. The feasibility was reviewed by analyzing the turbo compound speed, pressure drop, power generation, etc., using a one-dimensional simulation method. The maximum power generation of the configured turbo compound system was approximately 9 kW, and approximately 1–3 kW of energy could be recovered under medium speed and load conditions, which are the optimal operating conditions for a test engine with the displacement of a 4 L.

**Keywords:** exhaust energy recovery system; mobile carbon capture; turbo compound; 1D simulation



**Citation:** Woo, S.; Jeong, Y.; Lee, K. Feasibility Study of Exhaust Energy Recovery System for Mobile Carbon Capture Operations in Commercial Engines through 1D Simulation. *Energies* **2023**, *16*, 8025. <https://doi.org/10.3390/en16248025>

Academic Editors: Andrzej Ziółkowski, Paweł Fuć and Piotr Lijewski

Received: 24 November 2023

Revised: 7 December 2023

Accepted: 8 December 2023

Published: 12 December 2023



**Copyright:** © 2023 by the authors. Licensee MDPI, Basel, Switzerland. This article is an open access article distributed under the terms and conditions of the Creative Commons Attribution (CC BY) license (<https://creativecommons.org/licenses/by/4.0/>).

## 1. Introduction

Carbon emission regulations in major countries around the world are being strengthened. The European Union has finalized regulations on sales restrictions of internal combustion engine vehicles (ICEVs) after 2035 and has enacted legislation to reduce carbon dioxide (CO<sub>2</sub>) emissions by 50% compared to 2021 levels by 2030. Major countries, such as the United States, Japan, and China, are also aiming to reduce CO<sub>2</sub> emissions by 10–50% compared with conventional regulations [1–6]. As a result, the proportion of eco-friendly vehicles is increasing every year; however, if hybrid vehicles are included, the powertrain of vehicles in most countries still includes internal combustion engines (ICE); therefore, research on reducing carbon emissions from ICE is continuously required [7]. To respond to this situation, discussions are underway to achieve carbon neutrality of ICE by introducing electrofuels (e-fuels) that can replace conventional fossil fuels [8–10]. E-fuel is a synthetic fuel that can replace conventional fossil fuels and is manufactured by synthesizing green hydrogen and carbon dioxide captured through carbon capture utilization [11–13]. Therefore, to consider e-fuel as a carbon-neutral fuel, research on direct carbon capture (DAC) or mobile carbon capture (MCC) must be conducted together [14–17]. Finally, carbon neutrality of ICEVs is possible if e-fuel is supplied by synthesizing CO<sub>2</sub> captured from the tailpipe of a conventional ICE and green H<sub>2</sub>. Saravanan, S. evaluated whether CO<sub>2</sub> adsorption of small diesel engine exhaust gas was possible with zeolite 13X [14]. Sharma, S. presents a system for CO<sub>2</sub> capture from the exhaust stream of an internal combustion engine. Waste heat from exhaust gas was recovered through a Rankine cycle system to obtain energy for operating the system. Ultimately, it is expected that 90% of CO<sub>2</sub> contained in exhaust gas can be captured without external energy. However, dozens of heat

exchangers are required to configure the system, and the fixed composition and flow rate of the exhaust gas have been assumed, to calculate the heating/cooling requirements of the system. Therefore, operation in real conditions is impossible [15]. Voice, A. K. used ASPEN Plus V10 to evaluate the thermodynamic potential of carbon capture from internal combustion engines and consider engine exhaust gas heat energy to drive a small-scale carbon capture system [17]. Nevertheless, one of the biggest problems with e-fuels is that the energy required to operate the MCC system must be added to the vehicle system. In particular, to install and operate MCC under real conditions, the feasibility of the developed system must be reviewed under actual engine exhaust gas conditions. Therefore, in this study, a feasibility study of the actual engine operating conditions of an engine exhaust gas energy recovery system considering the installation of an MCC system was performed using a one-dimensional (1D) simulation method.

## 2. Experimental Setup and Procedure

### 2.1. Test Engine and Exhaust Energy Recovery System

A test engine was selected to review the feasibility of the specific-engine exhaust gas energy recovery system. From a long-term perspective, it is appropriate to consider an MCC system that can be installed in light-duty vehicles. However, considering the system installation space, the development is expected to be extremely difficult in the absence of a dedicated platform. In addition, the development of a system that can be installed on a vehicle currently in operation rather than on a vehicle to which a dedicated platform is applied will be more advantageous for practical use. Most leading researchers have verified the feasibility of the MCC system for Class 8 semi-trucks by considering the CO<sub>2</sub> emitted from the trucking industry and the system installation space [18]. In this study, a 2.5–3.5 ton payload capacity truck engine was selected to consider smaller-scale transportation, and its feasibility was verified. Table 1 lists the specifications of the test engine that satisfies euro-6D regulations.

**Table 1.** Specifications of the test engine.

Description	Specification
Type	Inline DOHC Euro-6D
Number of cylinders	4
Bore × Stroke [mm]	103 × 118
Displacement [cc]	3933
Compression ratio	17.1
Intake system	Various geometry turbocharger
Rated power [ps/rpm]	170/2500
Rated torque [kgf·m/rpm]	62/1400

Many studies have been conducted to increase engine efficiency by utilizing ICE waste energy. The representative waste energy from ICE is the exhaust gas energy. Technologies for its recovery include turbo compounds, the Rankine cycle, and thermoelectric power generation technology [19].

Turbo compounds are systems that can recover the kinetic and thermal energies of exhaust gases. Generally, when installed in the exhaust system of an ICE, the waste energy is converted into kinetic energy. It is most suitable for diesel engines and has the advantage of being easily installed in conventional ICEs. However, the exhaust gas pressure of the engine and the pumping loss increase, which poses a problem [20,21].

The Rankine cycle is a thermal energy recovery system that uses a working fluid through a phase change. In this structure, the working fluid is circulated in a closed circuit. The Rankine cycle is composed of a pump, boiler, condenser, and expander, and, therefore, its structure is complicated. It is most suitable for medium–low-temperature exhaust gas temperature conditions, and has the advantage of minimizing the effect on engine performance. However, the reactivity decreases under transient conditions. The

recovered energy is recovered as kinetic energy through an expander, and, in some cases, it is recovered electrically by coupling a generator [22,23].

A thermoelectric generator is a technology that recovers thermal energy by utilizing the Seebeck effect, which generates electricity when a temperature difference is applied to both ends of a module. Because there are no physically moving parts, it has the advantage of being lightweight and small in the system installation space. However, the disadvantage is that the price is relatively high, and the recovery efficiency is low because of the difference in power generation according to temperature conditions [24,25].

In this study, the application technology was determined by considering the installation, efficiency, cost, structure, and engine performance of each waste energy recovery system, as listed in Table 2. In particular, it was considered in the final installation that the waste energy recovery system and MCC system should be installed together. Finally, the electric turbo compound system was determined to be the most suitable for application in the MCC system.

**Table 2.** Characteristics of waste energy recovery system [19].

	Installation	Efficiency	Cost	Structure	Engine Performance	Note
Turbo compound	⊙	○	⊙	○	△	<ul style="list-style-type: none"> <li>• Best suited for diesel engine;</li> <li>• Simple installation on a conventional engine system;</li> <li>• Increase in exhaust back pressure and pumping loss.</li> </ul>
Rankine cycle	△	○	○	△	⊙	<ul style="list-style-type: none"> <li>• Best suited for mid–low exhaust gas temperature;</li> <li>• Highest number of parts;</li> <li>• Relatively low energy recovery efficiency;</li> <li>• Reactivity problem under transient conditions.</li> </ul>
Thermoelectric generator	⊙	△	△	⊙	⊙	<ul style="list-style-type: none"> <li>• No physically working parts;</li> <li>• Lightweight, small size;</li> <li>• Relatively high cost;</li> <li>• Efficiency change with temperature conditions;</li> <li>• Low energy recovery efficiency.</li> </ul>

△: Good, ○: better ⊙: Best

## 2.2. Turbo Compound System

As previously mentioned, a turbo-compound system is generally configured by installing a blowdown turbine in the ICE exhaust system. By classifying the installation methods in detail, they can be divided into four types, as shown in Figure 1. A serial or parallel turbo generator system is a method for installing a blowdown turbine in addition to a conventional turbocharger. The electric turbocharger/generator type installs a motor on the shaft of a conventional turbocharger. When turbo lag occurs, the impeller is forcibly rotated using an electric motor. When the turbine rotates sufficiently, the motor is used as a generator to recover the energy. The method in which the electric supercharger and turbo generator are installed separately can be considered ideal. The air required for the ICE is supplied by an electric supercharger. The turbo generator installed in the exhaust system is used only for power generation. However, complex control methods are required to operate these systems properly. In this study, a serial-type turbo generator was selected because it can be installed in the conventional engine system of a vehicle currently in operation.

As shown in Figure 2, the test engine was equipped with various exhaust gas post-processing systems to comply with emission regulations. The exhaust gas post-processing system of the test engine consists of a diesel oxidation catalyst (DOC), diesel particulate filter (DPF), selective catalytic reduction (SCR), and ammonia oxidation catalyst (AOC). Furthermore, a hydro carbon injection (HCI) is installed separately. The recoverable energy increased when the installation location of the turbo compound was close to that of the test engine. However, problems may occur if the exhaust gas is not processed by the exhaust gas post-processing system. Since Point ① is closest to the engine, it can recover the most kinetic energy and thermal energy of the exhaust gas. In the case of Point ②, the conditions

are similar to those of Point ①; however, problems may occur in the impeller owing to the fuel injected under the HCl operating conditions. Point ③ can be affected by ammonia sprayed by the urea dosing nozzle installed downstream of the DPF. Point ④ has the lowest recoverable energy, and installation of the MCC system is considered. Therefore, point ① was selected as the installation location of the turbo compound system, as that can increase the efficiency of the turbine the most [26].

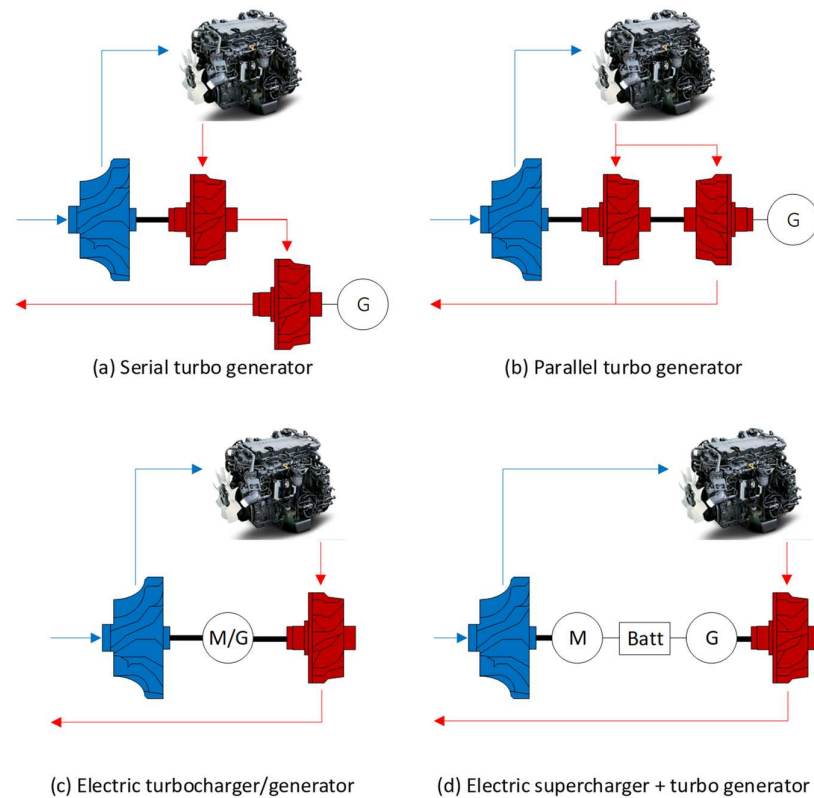
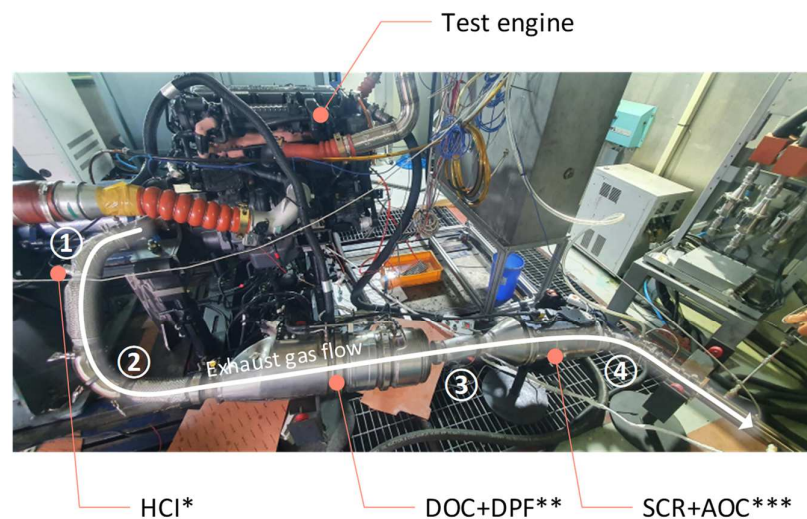


**Figure 1.** Various types of electric turbo compounding system (M: motor, G: generator).



\*HCl: Hydro carbon injection

\*\*DOC+DPF: Diesel oxidation catalyst + Diesel particulate filter

\*\*\*SCR+AOC: Selective catalytic reduction + Ammonia oxidation catalyst

**Figure 2.** Exhaust gas post processing system of the test engine.

The electric turbo compound considered in this study consisted of a turbine for waste exhaust gas energy recovery and a power generation system for converting the recovered energy into electricity. The turbine must have high efficiency at a low pressure ratio to minimize the decrease in the efficiency of the ICE owing to the increase in exhaust gas back pressure. The generator system must be highly efficient under the turbine operating conditions. In addition, because the specifications of the test engine have been determined, the turbine and generating system must be selected based on the operating conditions of the test engine.

The test engine, with a displacement of 4 L, was equipped with a conventional turbocharger. Therefore, assuming that the exhaust gas energy is primarily recovered by the conventional charging system, the turbine specification of a 2 L displacement diesel engine was applied to the turbo compound system. The selected turbine rotated at tens of thousands of rpm when it was operated normally under the exhaust gas conditions of the test engine. Therefore, a synchronous generator with the specifications listed in Table 3, capable of a high revolution rate, was selected. The maximum number of revolutions was 120,000 rpm, and the power generation was 10 kW. The output increases linearly with the number of revolutions. For comparison with the selected synchronous generator, the heavy-duty alternator listed in Table 4 was selected and considered for application. The maximum revolution speed is 8000 rpm, and the maximum output is about 6.8 kW at an ambient temperature of 110 °C. In addition, in the case of the alternator, the product is already equipped with a rectifier and regulator, so there is an advantage in that it can be applied immediately without additional equipment. Because both cases have advantages and disadvantages, 1D simulations were conducted for the two types of methods with different specifications.

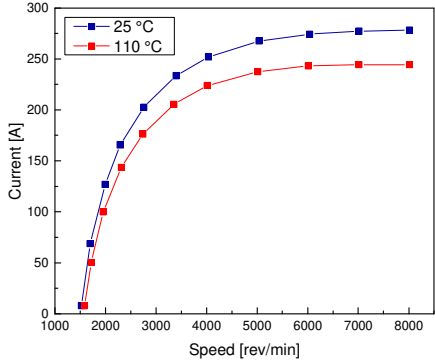
**Table 3.** Specifications of the synchronous generator.

Description	Specification
Maximum speed [rev/min]	120,000 (continuous)
Apparent power [kVA]	10.8
Power [kW]	10
Voltage [V]	348
Current [A]	18
Frequency [hz]	2000
Performance	

Speed [rev/min]	Torque [Nm]	Power [kW]
0	0.83	0
20,000	0.83	1.67
40,000	0.83	3.33
60,000	0.83	5.00
80,000	0.83	6.67
100,000	0.83	8.33
120,000	0.83	10.00

**Table 4.** Specifications of the heavy-duty alternator.

Description	Specification
Maximum speed [rev/min]	8000 (continuous) 9000 (intermittent)
Voltage [V]	24
Current [A]	275
Efficiency [%]	>80
Performance	

### 2.3. Test Conditions

The World Harmonized Stationary Cycle (WHSC) was considered a test condition other than the full load condition of the target engine. The WHSC is a steady-state engine dynamometer test cycle for heavy-duty engines. Detailed operating conditions are listed in Table 5, in which the data were obtained after a stabilization period of 10 min or more for each condition.

**Table 5.** WHSC test conditions.

Mode	Engine Speed		Engine Torque	
	%	rpm	%	Nm
1	0	650	0	0
2	55	2050	100	545
3	55	2050	25	140
4	55	2050	70	395
5	35	1750	100	580
6	25	1600	25	145
7	45	1900	70	405
8	45	1900	25	145
9	55	2050	50	280
10	75	2350	100	475
11	35	1750	50	295
12	35	1750	25	150
13	0	650	0	0

### 2.4. 1D Simulation Model

SIEMENS' advanced modeling environment for the simulation of engineering systems (AMESim) was used to predict the performance of the components and turbo-compound systems. A simulation model was developed to predict the speed, torque, power generation, and energy recovery efficiency of the turbo-compound system based on the temperature and flow rate of the exhaust gas of the test engine. The turbine was modeled by referring to the turbocharger applied to the 2 L diesel engine. The turbine model was set up using the turbocharger map-processing tool provided by AMESim 2210. As shown in Table 6, the turbine map was derived according to the input values, with multidimensional data consisting of five variables: the variable geometry turbocharger (VGT) position and reduced speed. In addition, directly measurable turbine hardware specifications were applied.

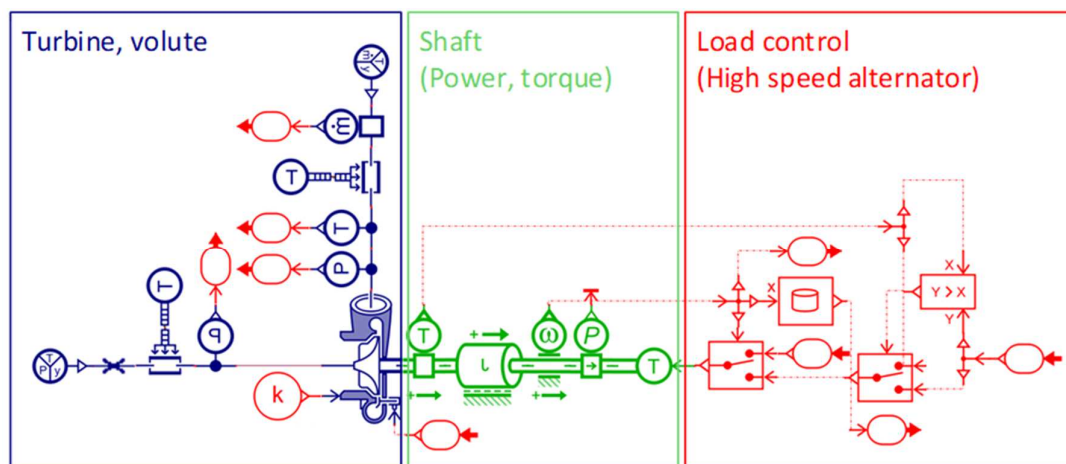
**Table 6.** Parameters of the turbine map.

Parameter	Unit
VGT position	-
Reduced rotary speed ( $N_{\text{reduce}}$ )	rpm/ $\sqrt{K}$
Reduced mass flow rate ( $\dot{m}_{\text{reduce}}$ )	kg/s $\cdot\sqrt{K}$ /kPa
Pressure ratio	-
Isentropic efficiency	-

$N_{\text{reduce}} = N_{\text{actual}}/\sqrt{T_{\text{up}}}$ ,  $\dot{m}_{\text{reduce}} = \dot{m}_{\text{actual}}\cdot\sqrt{T_{\text{up}}}/P_{\text{up}}$ ,  $T_{\text{up}}$  : upstream temperature[K],  $P_{\text{up}}$  : upstream pressure[kPa].

The model was configured differently depending on the type of generator system, and the analysis was conducted by configuring the model in two cases. Case 1 uses a high-speed synchronous generator, and Case 2 uses a relatively low-speed heavy-duty alternator. However, in Case 2, because the maximum rotational speed of the target alternator was 8000 rpm, a rotation speed reducer was configured on the shaft to adjust the rotational speed.

In Case 1, the power and torque had linear values depending on the number of revolutions. The model was constructed so that the expected power generation could be derived from the input torque under steady conditions. The generator model is interlocked with the turbine model to form a turbo-compound simulation model, as shown in Figure 3.

**Figure 3.** Turbo compound 1D simulation model (Case 1, generator model).

Because the heavy-duty alternator applied to the Case 2 model did not produce a constant output depending on the number of revolutions, a separate generator model was used to derive the map data and apply it to the simulation model. The derived map data are verified using a specification sheet. For torque, an error of less than 3% and an output of less than 1% were considered usable. Therefore, as shown in Figure 4, a simulation model was constructed by combining it with the turbine model. In addition, as mentioned above, a rotation speed reducer was configured on the drive shaft to adjust the number of revolutions with a gear ratio of 1–50:1 according to the driving conditions.

The energy-recovery performance of the turbo compound system in the test engine was predicted using a configured 1D simulation model. For the input parameters, the exhaust gas conditions measured according to the operating conditions were applied through the base performance evaluation of the test engine. Accordingly, as shown in Table 7, the turbine speed, pressure drop, and power generation were acquired and analyzed. The turbo compound speed can be identified from the rotational speed of the turbine, and the increase in the exhaust gas backpressure of the test engine can be inferred from the turbine pressure drop value. The power generation and energy recovery rate of the turbo compound were

measured using the equations in Table 7 and used as performance evaluation indicators of the turbo compound according to the operating conditions [27].

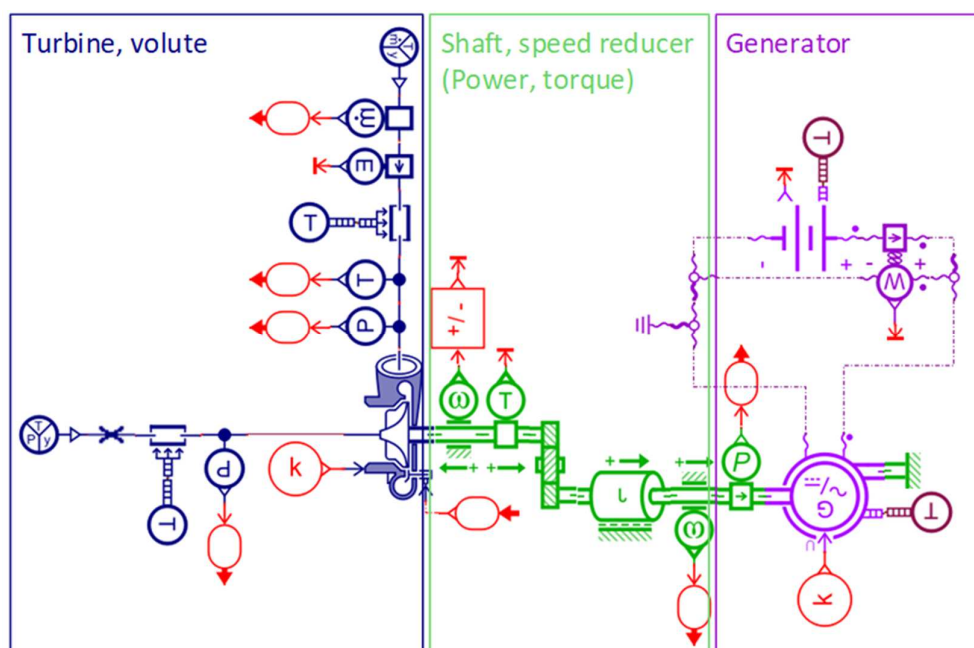


**Figure 4.** Turbo compound 1D simulation model (Case 2, alternator model with rotation speed reducer).

**Table 7.** Parameters of the simulation model.

Input Parameters		Output Parameters	
Description	Unit	Description	Unit
Exhaust gas mass flow rate	kg/h	Turbine speed	rpm
Exhaust gas temperature	°C	Turbine pressure drop	bar
		Power generation	kW
		Energy recovery rate	%

$$E_{\text{exhaust}} = m_{\text{exhaust}} C_p \Delta T_{\text{exhaust}}, \text{ Energy recovery rate}[\%] = E_{\text{turbo compound}} / E_{\text{exhaust}} \times 100.$$

### 3. Results and Discussion

#### 3.1. Exhaust Gas Properties of Test Engine

Before proceeding with the simulation to predict the performance of the turbo-compound system, a base performance evaluation of the test engine was conducted. Based on the base performance evaluation, the characteristics of the exhaust gas temperature and flow rate according to the operating conditions were analyzed to identify the conditions under which the turbo compound operates. Figure 5 is the exhaust gas temperature according to the operating conditions of the test engine. The exhaust gas temperature ranges from 110 to 460 °C, and increases with increasing engine load. The exhaust gas mass flow rate was calculated by adding the air and fuel flow rates supplied to the test engine, and the measurement results are shown in Figure 6. The exhaust gas mass flow rate ranged from 73 kg/h to 660 kg/h, and increased with increasing engine speed and load. The exhaust gas energy of the test engine was analyzed based on the measured exhaust gas temperature and flow rate. Figure 7 shows the exhaust gas energy of the test engine according to the operating conditions. Among the WHSC mode conditions for evaluating heavy-duty engines, the energy of the exhaust gas is more than 40 kW under medium–high load conditions. However, as shown in Figure 8, assuming that the pressure ratio of the

turbo-compound system is 1.3, the actual recoverable energy is expected to be less than 10 kW.

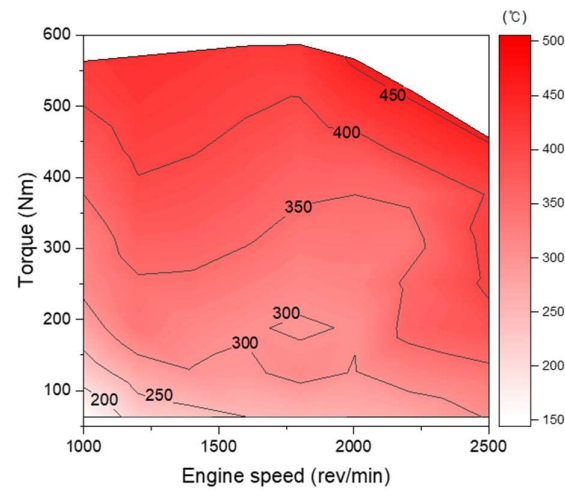


Figure 5. Exhaust gas temperature of test engine according to operating conditions.

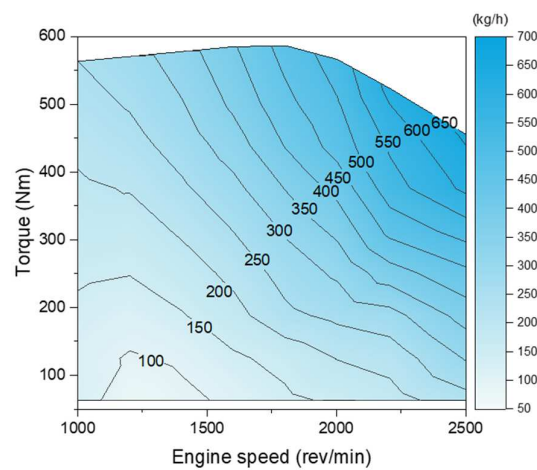


Figure 6. Exhaust gas mass flow rate of test engine according to operating conditions.

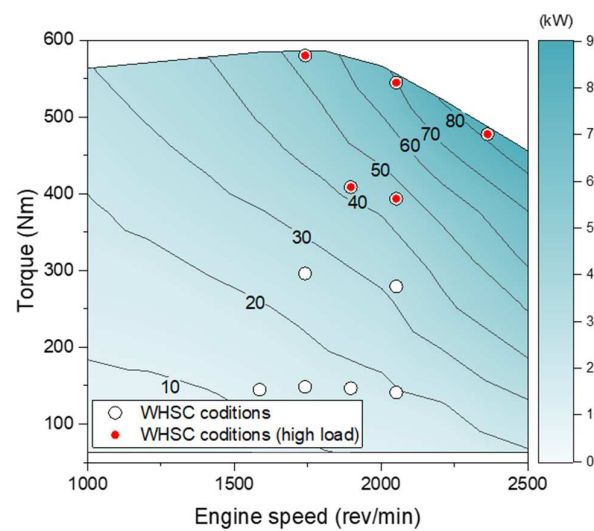
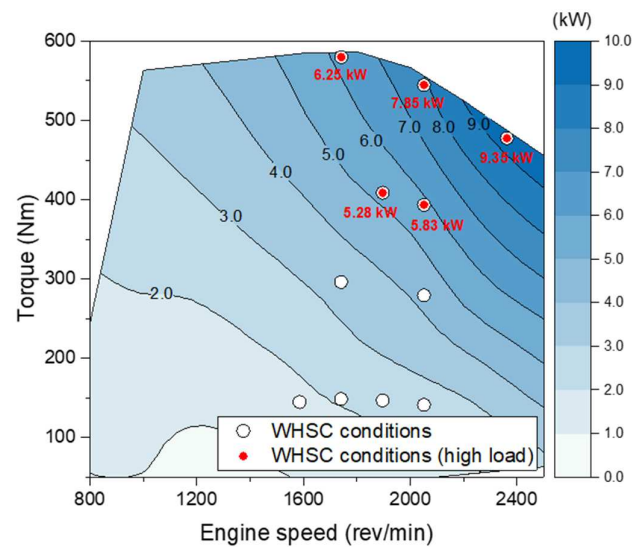


Figure 7. Exhaust gas energy of the test engine according to operating conditions.



**Figure 8.** Power output of engine exhaust gas (total pressure ratio = 1.3).

### 3.2. Simulation Results of Turbo Compound System

In order to predict the performance of the configured turbo compound model, the performance prediction results of the analysis model were derived under the conditions of gas temperature 100–600 °C and flow rate 0–600 kg/h. Because the generator speed specification of Case 1 is 125,000 rpm and the torque is as low as 0.8 Nm, it is predicted that an energy recovery of up to 8 kW is possible, as shown in Figure 9. In Case 2, the maximum revolution speed of the alternator was less than 9000 rpm, and the maximum power generation was 6.8 kW. Furthermore, the result was derived as shown in Figure 10. In addition, because there is a difference in the torque according to the operating conditions, the speed change according to the gas conditions is small. The maximum power generation is lower than that in Case 1, but it is expected to utilize up to 6.8 kW, which is the maximum performance of the alternator.

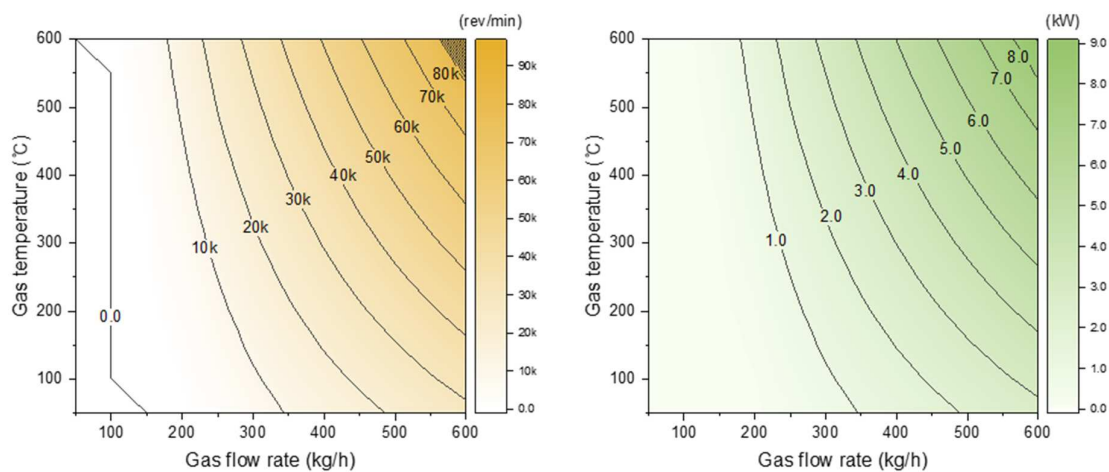


**Figure 9.** Speed (left) and power (right) of turbo compound according to operating conditions (Case 1, generator model).

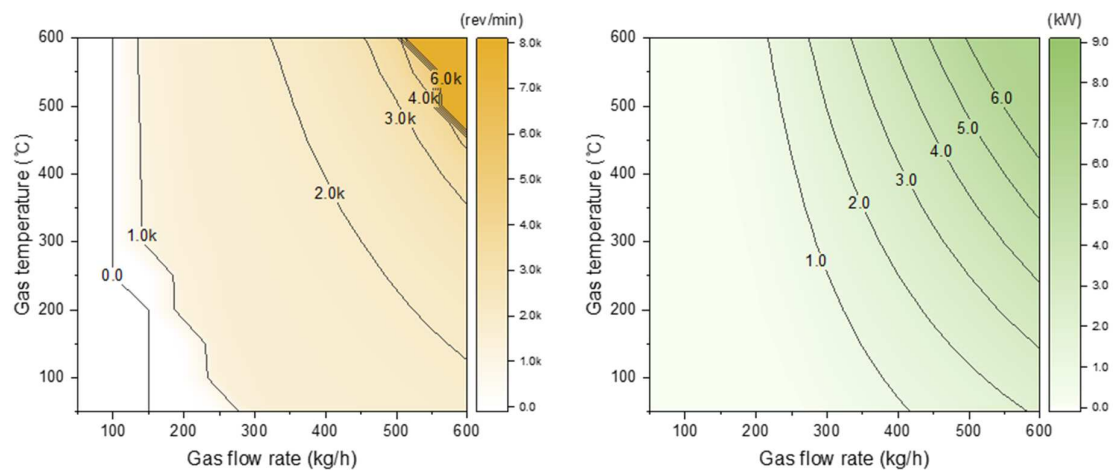


**Figure 10.** Speed (left) and power (right) of turbo compound according to operating conditions (Case 2, alternator model).

The feasibility was verified by applying the exhaust gas conditions of the test engine to a previously reviewed turbo-compound performance prediction model. Based on the exhaust gas property results, gas conditions according to the engine speed and load were applied, and Cases 1 and 2 were applied and compared. Figures 11 and 12 show the turbo compound speed results based on the operating conditions. Similar to the previous results, the number of revolutions in Case 1 increased according to the engine speed and load. In Case 2, the turbo compound speed increased very slowly under medium–low load conditions. This means that a section with a high alternator efficiency cannot be used under the operating conditions of the test engine. Therefore, to apply the alternator in Case 2, it is essential to apply a dedicated low-speed, low-pressure turbine or a rotation speed reducer [28].

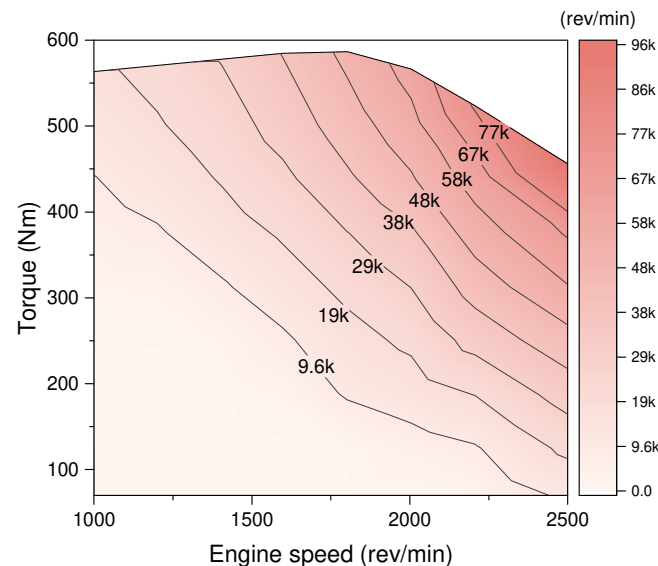


**Figure 11.** Speed of turbo compound according to engine conditions (Case 1, generator model).

The pressure drop in a turbo compound system can directly affect the performance of the test engine by increasing the exhaust gas back pressure. A large pressure drop indicates that the exhaust back pressure of the engine increases, which is directly related to an increase in the pumping loss. Figures 13 and 14 show the pressure drops of the turbo compound according to the operating conditions. In both cases, the pressure drop increased in proportion to the engine speed and torque, and in Case 1, a larger pressure drop occurred. In addition, in both cases, a pressure drop of more than 0.6 bar occurs

under high load conditions in WHSC mode, so a method to compensate for this is required. However, the pressure drop was as low as 0.5 bar or less in all cases under medium–low speed conditions. In Case 2, the pressure drop was less than that in Case 1; therefore, the effect on engine performance was expected to be less. Nevertheless, it is necessary to select the optimal operating conditions by matching the operating range of the turbo compound with the engine exhaust gas conditions.

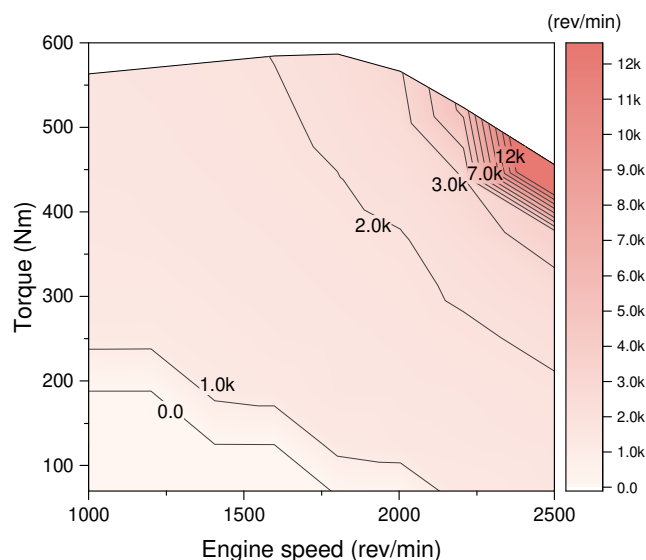


**Figure 12.** Speed of turbo compound according to engine conditions (Case 2, alternator model).

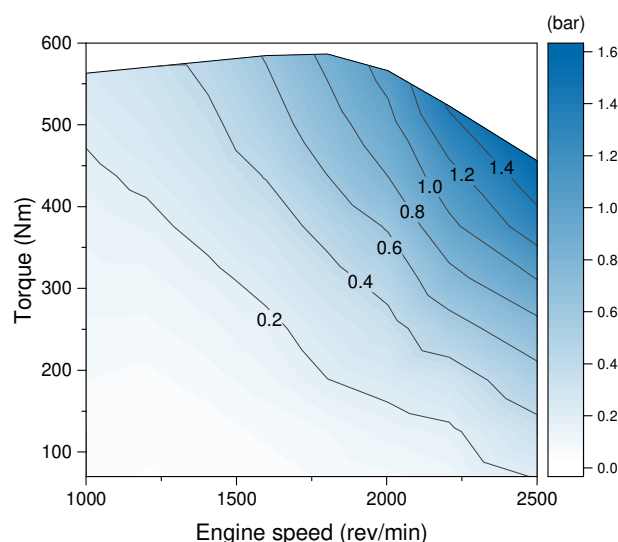


**Figure 13.** Pressure drop of turbo compound according to engine conditions (Case 1, generator model).

Figures 15 and 16 show the expected power generation of the turbo compound for each case, according to the engine operating conditions. The maximum power generation in Case 1 is superior to that in Case 2 by approximately 2.5 kW. In Case 1, the maximum power generation was approximately 9 kW, and the energy recovery rate was approximately 10%. The maximum power generation in Case 2 was approximately 6.5 kW, and the energy recovery rate was approximately 7%; This is the result of the difference in specifications between the generator applied in Case 1 and the alternator applied in Case 2. However, because the difference in power generation under each condition of the WHSC mode, which is the actual operating condition, is less than the maximum value of 1 kW, the difference in performance is much smaller than the difference in the specifications. Under

medium-speed and medium-load conditions, Case 1 generated 1–3 kW with an energy recovery rate of 6–8%. In contrast, Case 2 generated 1–2 kW, and the energy recovery rate was 4–6%. The maximum recovery rate was not significantly different compared with the difference between the maximum power generation and the specifications. In addition, because the pressure drop is small, the performance can be improved by adjusting the system hardware [20].

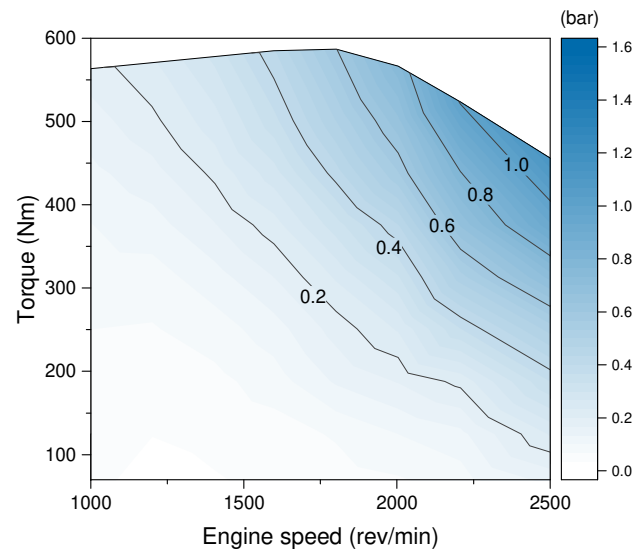


**Figure 14.** Pressure drop of turbo compound according to engine conditions (Case 2, alternator model).

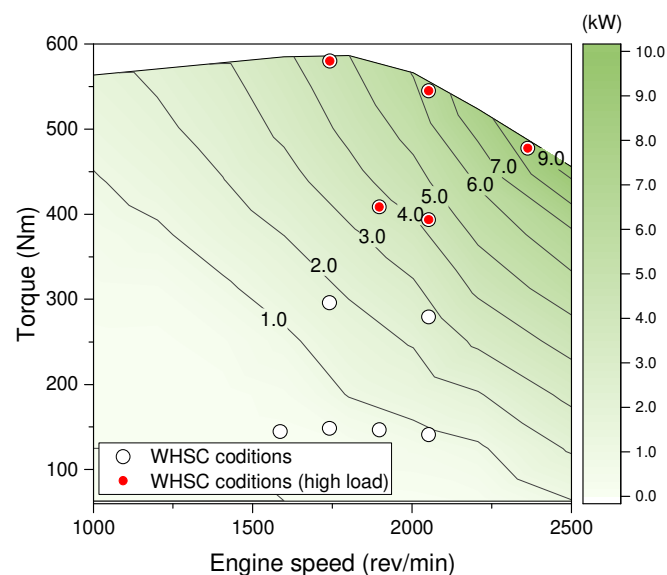


**Figure 15.** Turbo compound power according to engine conditions (Case 1, generator model).

The maximum rotational speed of the alternator in Case 2 was 8000 rpm, which was much lower than the operating range of the turbine; therefore, this effect was analyzed by applying a rotational speed reducer. Figure 17 shows the analysis results for the turbo compound Case 2 when the rotation speed reducer was applied. The engine operating conditions applied two, four, and seven modes, which are relatively high-load conditions, among the WHSC modes. The difference in power generation due to the rotation speed reducer appeared at 25–40:1 or more. The power generation was the maximum at 25:1 under WHSC 2 conditions and 40:1 under WHSC 4 and 7. It is possible to improve the power generation performance by applying a rotational speed reducer. However, since the ratio is large, it is expected that it will be almost impossible to apply in real-world

conditions. Even in this case, it is necessary to apply a low-speed turbine considering the alternator speed conditions.

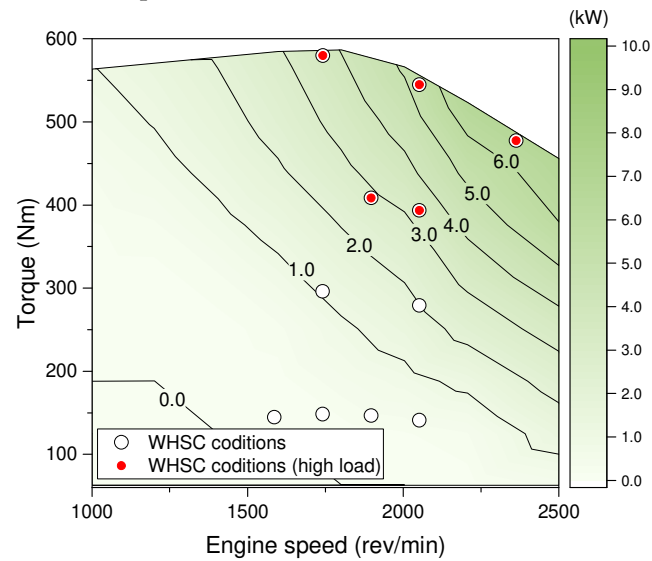


**Figure 16.** Turbo compound power according to engine conditions (Case 2, alternator model).

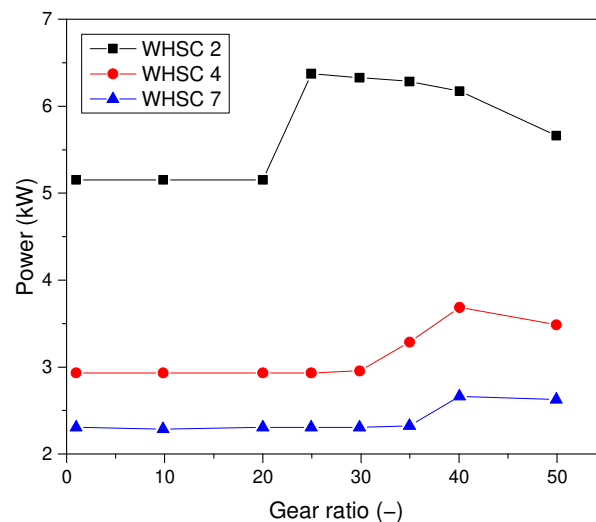


**Figure 17.** Turbo compound power variation according to rotation speed reduction gear ratio.

#### 4. Conclusions

In this study, based on a 4 L diesel engine, exhaust gas characteristics were analyzed according to operating conditions. A waste energy recovery system suitable for the test engine was selected, and element parts were configured. The waste exhaust gas energy recovery performance and optimal operating conditions of the turbo compound system were analyzed using a 1D simulation method, and the following conclusions were drawn:

1. The exhaust gas temperature of test engine is distributed between 110 and 460 °C and increases with engine load. The exhaust gas flow rate is distributed between 73 and 660 kg/h and increases with engine speed and engine load. The exhaust gas of the target engine has energy of up to 40 kW, but the recoverable energy at the turbo compound's pressure ratio of 1.3 is up to 10 kW or less.
2. Regarding installing an MCC system, the most suitable waste energy recovery system for the test engine is an electric turbo compound system. The simulation is divided into Case 1 (high-speed synchronous generator) and Case 2 (heavy-duty alternator). In Case 1, the rotation speed increases linearly up to 90,000 rpm depending on the

operating conditions. In Case 2, the rotation speed rapidly increases to 120,000 rpm under high load conditions, exceeding the specification limit, so the application of a reducer or low speed turbine is necessary.

3. Turbo compound pressure drop is up to 1.4 bar in Case 1 and up to 1.0 bar in Case 2, which is about 50% higher than Case 1. However, the pressure drop in the medium-speed and -load conditions is below 0.2–0.6 bar in both cases. Therefore, in order to maximize the performance of the test engine and optimize the efficiency of the turbo compound, it is necessary to apply a low pressure turbine.
4. The maximum power generation according to engine operating conditions is about 9 kW for Case 1 and 6.5 kW for Case 2, with Case 1 being superior by about 2.5 kW. However, when compared in WHSC conditions, the difference in power generation is less than 1 kW. In Case 2, the pressure drop performance is better than Case 1, so performance can be improved by improving hardware.
5. Considering the maximum speed of the heavy-duty alternator in Case 2, a speed reducer was applied to optimize power generation. Although the power generation is improved when the speed reducer ratio is 25:1 or higher, the reduction ratio is at a level that is difficult to consider real conditions. Therefore, it is expected that performance improvement will be possible by applying a low speed turbine with high efficiency under the same conditions as the optimal operating conditions of the generator.

By applying the turbo compound system composed of a 1D simulation model to a test engine, the feasibility of recovering more than 1–3 kW of energy while minimizing the impact on engine performance was confirmed. To improve performance, additional research is needed on high-speed rotation speed reducers or low-speed, low-pressure turbines, etc.

**Author Contributions:** Conceptualization, S.W. and K.L.; methodology, S.W.; software, Y.J.; validation, S.W. and Y.J.; formal analysis, S.W.; investigation, S.W. and Y.J.; resources, K.L.; data curation, Y.J.; writing—original draft preparation, S.W.; writing—review and editing, S.W.; visualization, Y.J.; supervision, K.L.; project administration, K.L.; funding acquisition, K.L. All authors have read and agreed to the published version of the manuscript.

**Funding:** This work was supported by the Technology Innovation Program (or Industrial Strategic Technology Development Program) (20018346, Development of an adsorption-desorption system to capture carbon dioxide emitted from commercial vehicles) funded By the Ministry of Trade, Industry & Energy (MOTIE, Sejong-si, Republic of Korea).

**Data Availability Statement:** The data presented in this study are available on request from the corresponding author.

**Conflicts of Interest:** The authors declare no conflict of interest.

## References

1. Conway, G.; Joshi, A.; Leach, F.; García, A.; Senecal, P.K. A review of current and future powertrain technologies and trends in 2020. *Transp. Eng.* **2021**, *5*, 100080. [[CrossRef](#)]
2. Continental, A. *Worldwide Emission Standards and Related Regulations*; Continental Automotive GmbH: Regensburg, Germany, 2019.
3. Wallington, T.J.; Sullivan, J.L.; Hurley, M.D. Emissions of CO<sub>2</sub>, CO, NO<sub>x</sub>, HC, PM, HFC-134a, N<sub>2</sub>O and CH<sub>4</sub> from the global light duty vehicle fleet. *Meteorol. Z.* **2008**, *17*, 109–116. [[CrossRef](#)]
4. Greene, D.L.; Baker, H.H., Jr.; Plotkin, S.E. *Reducing Greenhouse Gas Emissions from US Transportation*; Pew Center on Global Climate Change: Arlington, VA, USA, 2010.
5. Hankey, S.; Marshall, J.D. Impacts of urban form on future US passenger-vehicle greenhouse gas emissions. *Energy Policy* **2010**, *38*, 4880–4887. [[CrossRef](#)]
6. Kyle, P.; Kim, S.H. Long-term implications of alternative light-duty vehicle technologies for global greenhouse gas emissions and primary energy demands. *Energy Policy* **2011**, *39*, 3012–3024. [[CrossRef](#)]
7. Harrison, D. Automotive powertrain forecast 2020–2030 navigating regional and regulatory divergence on the road to electrification. In *Automotive from Ultimamedia*; Oracle: Austin, TX, USA, 2019.

8. Pearson, R.J.; Eisaman, M.D.; Turner, J.W.G.; Edwards, P.P.; Jiang, Z.; Kuznetsov, V.L.; Littau, K.A.; Di Marco, L.; Taylor, S.R.G. Energy Storage via Carbon-Neutral Fuels Made from CO<sub>2</sub>, Water, and Renewable Energy. *Proc. IEEE* **2012**, *100*, 440–460. [[CrossRef](#)]
9. Ramirez, A.; Sarathy, S.M.; Gascon, J. CO<sub>2</sub> Derived E-Fuels: Research Trends, Misconceptions, and Future Directions. *Trends Chem.* **2020**, *2*, 785–795. [[CrossRef](#)]
10. Maas, H.; Schamel, A.; Weber, C.; Kramer, U. Review of combustion engine efficiency improvements and the role of e-fuels. In *Internationaler Motorenkongress 2016: Mit Konferenz Nfz-Motorentechnologie*; Springer: Wiesbaden, Germany, 2016; pp. 463–483.
11. Choi, Y.H.; Jang, Y.J.; Park, H.; Kim, W.Y.; Lee, Y.H.; Choi, S.H.; Lee, J.S. Carbon dioxide Fischer-Tropsch synthesis: A new path to carbon-neutral fuels. *Appl. Catal. B Environ.* **2017**, *202*, 605–610. [[CrossRef](#)]
12. Zang, G.Y.; Sun, P.P.; Yoo, E.; Elgowainy, A.; Bafana, A.; Lee, U.; Wang, M.; Supekar, S. Synthetic Methanol/Fischer-Tropsch Fuel Production Capacity, Cost, and Carbon Intensity Utilizing CO<sub>2</sub> from Industrial and Power Plants in the United States. *Environ. Sci. Technol.* **2021**, *55*, 7595–7604. [[CrossRef](#)]
13. Jones, M.P.; Krexner, T.; Bismarck, A. Repurposing Fischer-Tropsch and natural gas as bridging technologies for the energy revolution. *Energy Convers. Manag.* **2022**, *267*, 115882. [[CrossRef](#)]
14. Saravanan, S.; Kumar, C.R. Carbon Dioxide Capture using Adsorption Technology in Diesel Engines. *Int. J. Renew. Energy R.* **2020**, *10*, 1614–1620.
15. Sharma, S.; Marechal, F. Carbon Dioxide Capture from Internal Combustion Engine Exhaust Using Temperature Swing Adsorption. *Front. Energy Res.* **2019**, *7*, 143. [[CrossRef](#)]
16. Garcia-Mariaca, A.; Llera-Sastresa, E. Review on Carbon Capture in ICE Driven Transport. *Energies* **2021**, *14*, 6865. [[CrossRef](#)]
17. Voice, A.K.; Hamad, E. Evaluating the thermodynamic potential for carbon capture from internal combustion engines. *Transp. Eng.* **2022**, *10*, 100144. [[CrossRef](#)]
18. Voice, A.; Hamad, E. Mobile carbon capture for long-haul commercial transport: Design, integration and results. In Proceedings of the 16th Greenhouse Gas Control Technologies Conference (GHGT-16), Lyon, France, 23–24 October 2022.
19. Bai, S.X.; Liu, C.H. Overview of energy harvesting and emission reduction technologies in hybrid electric vehicles. *Renew. Sustain. Energy Rev.* **2021**, *147*, 111188. [[CrossRef](#)]
20. Aghaali, H.; Ångström, H.E. A review of turbocompounding as a waste heat recovery system for internal combustion engines. *Renew. Sustain. Energy Rev.* **2015**, *49*, 813–824. [[CrossRef](#)]
21. Arav, B.; Shulman, R.; Dooun, V. Basic Concepts for Forcing of Low-Power Micro Turbine Generators. *Procedia Eng.* **2016**, *150*, 1384–1390. [[CrossRef](#)]
22. Mahmoudi, A.; Fazli, M.; Morad, M.R. A recent review of waste heat recovery by Organic Rankine Cycle. *Appl. Therm. Eng.* **2018**, *143*, 660–675. [[CrossRef](#)]
23. Lee, J.; Choi, K.; Lee, K.; Shin, K. Parametric study of the effects of the design factors on the performance of a heat recovery system obtained from an exhaust gas in a gasoline engine. *Proc. Inst. Mech. Eng. Part D J. Automob. Eng.* **2014**, *228*, 1568–1580. [[CrossRef](#)]
24. In, B.D.; Kim, H.I.; Son, J.W.; Lee, K.H. The study of a thermoelectric generator with various thermal conditions of exhaust gas from a diesel engine. *Int. J. Heat Mass Transf.* **2015**, *86*, 667–680. [[CrossRef](#)]
25. Burnete, N.V.; Mariasiu, F.; Depcik, C.; Barabas, I.; Moldovanu, D. Review of thermoelectric generation for internal combustion engine waste heat recovery. *Prog. Energy Combust. Sci.* **2022**, *91*, 101009. [[CrossRef](#)]
26. Lambert, C.; Hammerle, R.; Kubinski, D.; Levin, M. Urea SCR and DPF system for diesel sport utility vehicle meeting Tier 2 bin 5. In Proceedings of the US Department of Energy Diesel Engine Emissions Reduction (DEER) Conference, Chicago, IL, USA, 21–25 August 2005.
27. Nonthakarn, P.; Ekpanyapong, M.; Nontakaew, U.; Bohez, E. Design and Optimization of an Integrated Turbo-Generator and Thermoelectric Generator for Vehicle Exhaust Electrical Energy Recovery. *Energies* **2019**, *12*, 3134. [[CrossRef](#)]
28. Bin Mamat, A.M.I.; Martinez-Botas, R.F.; Rajoo, S.; Romagnoli, A.; Petrovic, S. Waste heat recovery using a novel high performance low pressure turbine for electric turbocompounding in downsized gasoline engines: Experimental and computational analysis. *Energy* **2015**, *90*, 218–234. [[CrossRef](#)]

**Disclaimer/Publisher’s Note:** The statements, opinions and data contained in all publications are solely those of the individual author(s) and contributor(s) and not of MDPI and/or the editor(s). MDPI and/or the editor(s) disclaim responsibility for any injury to people or property resulting from any ideas, methods, instructions or products referred to in the content.